Journal of Russian Laser Research, Volume 18, Number 1, 1997

DYNAMICAL COMPLEXITY OF DRIVEN TWO-LEVEL SYSTEMS. II. DYNAMICAL DRIVING BY A SELF-CONSISTENT RADIATION FIELD

S. V. Prants

Pacific Oceanological Institute, Russian Academy of Sciences, Baltijskaya 43, 690041 Vladivostok, Russia

Abstract

An ensemble of two-level radiators in a lossless cavity is considered as interacting with a resonant eigenmode field taking into account the feedback effect of the radiators on the field. In a semiclassical approximation, this dynamical system is described by the Maxwell–Bloch equations and is shown to have two control parameters, namely, the individual and cooperative Rabi frequencies. In the neoclassical Jaynes–Cummings treatment, a pure quantum-level description is converted to a set of closed c-number equations for quantum expectation values with a single control parameter (the cooperative vacuum Rabi frequency). We develop also a group-theoretical description for both of these models, which provides further insight into the general dynamic behavior. Increasing one of the model's control parameters, we investigate numerically the onset of dynamical chaos in field–atom interaction by calculating the maximum Lyapunov exponent of the Maxwell–Bloch and the Jaynes–Cummings dynamical systems. The onset is shown to differ depending on the model adopted, the control parameter used, and the initial conditions chosen. Possible candidates for experimentally observable (semi)quantum chaos in a system of dynamically driven two-level radiators are discussed by estimating the orders of magnitudes for the respective control parameters in actual quantum electrodynamical systems. It is shown that quantum-well excitons in fabricated semiconductor microcavities are likely candidates for experimental confirmation of transitions to dynamical chaos which have been revealed numerically in this study.

1. Introduction

In the preceding paper [1], a comprehensive analysis of the general dynamic behavior of an externally driven two-level atom in the context of dynamical-system theory was carried out using the properties of the underlying $SU(2)$ symmetry. In the present paper, we will consider dynamically driven two-level atoms in a cavity within the same context. From an abstract point of view, this coupled system provides a physical realization of an $SU(2)$ dynamical system driven by another dynamical system, namely, by a linear oscillator. Physically, this means that we take into account here the response of atoms to a radiation field in a resonant cavity.

As was shown in [1], the temporal evolution of a two-level atom in a given laser field is not truly chaotic. It may be more or less irregular, depending on the type of field polarization and on the ratio of the two driving frequencies. It may even result in broadened power spectra and phase portraits that appear quite irregular. However, the characteristic Lyapunov exponents are invariably nonpositive.

To evaluate the chaos, one needs to use the Lyapunov exponents for trajectories in a phase space of a dynamical system. For an n-dimensional dynamical system, there are n, possibly indistinguishable, Lyapunov exponents λ_j $(j = 1, 2, ..., n)$. By definition, we have [2]

$$\lambda = \lim_{t\to\infty} \lambda(t) , \quad \lambda(t) = \lim_{\Delta(0)\to 0} \frac{1}{t} \ln\left(\frac{\Delta(t)}{\Delta(0)}\right) , \tag{1}$$

Translated from a manuscript submitted December 25, 1995.

1071-2836/97/1801-0069$18.00

where $\Delta(t)$ is the distance between two initially adjacent trajectories at time t. These characteristics describe the exponential divergence or convergence of nearby trajectories. It follows from Eq. (1) that small deviations $\Delta(0)$ in initial conditions evolve in time as $\Delta(0)\exp\lambda t$. For regular motion, all the Lyapunov exponents vanish asymptotically in time. For chaotic motion in Hamiltonian dynamical systems, there exists at least one λ_j that is greater than zero for a reasonably long time. A positive value of λ implies an exponential separation in time of trajectories and, thus, dynamical chaos in the system.

In this paper, we consider an ensemble of two-level atoms in a single-mode high-Q cavity with the feedback effect of the atoms on the radiation field taken into account. To describe the atom–field interaction with the feedback, we must add an equation of motion for the field variables to the equations of motion for the atomic variables. It may be done in different ways.

In a semiclassical approximation (Sec. 2), the radiation field is treated *ab initio* as a classical one and is defined by the Maxwell equation. The other way is to start with a completely quantized Jaynes–Cummings Hamiltonian of the atom–field interaction and then to factorize the respective Heisenberg equations (Sec. 3). Such a procedure is referred to as a "neoclassical approximation" [3].

In the two-level case to be considered here, the atomic dynamics may be described by Bloch equations or by a second-order differential equation for the probability amplitudes in the Schrödinger picture or by a second-order differential equation for the $SU(2)$ group parameter in the group-theoretical picture. All these descriptions are, of course, equivalent. The language of the components of the Bloch vector and of the probability amplitudes is preferable from the physical point of view. However, the group-theoretical language is more general and enables one to describe consistently dynamical systems of a different nature. We will supplement the analysis of both the Maxwell–Bloch model and the Jaynes–Cummings model by corresponding group-theoretical descriptions (see Subsecs. 2.2 and 3.2). It will be shown in these subsections that the group-theoretical picture provides further insight into the dynamics of atom–field interaction in a cavity.

A brief review of actual quantum electrodynamical systems with strong coupling between the radiators and the cavity field is given in Sec. 4. From an estimate of the magnitude of this coupling it follows that the cavity polaritons in fabricated semiconductor microcavities are good candidates for experimental studies of transitions to (semi)quantum dynamical chaos.

2. The onset of Dynamical Chaos in a Semiclassical Model of Atom–Field Interaction

2.1. Maxwell–Bloch Dynamical System

The model involves a gaseous sample of N identical non-interacting two-level atoms with transition frequency ω and transition electric dipole moment d in a high-Q resonator with a single eigenmode which is assumed to be uniform along the resonator length. For simplicity, the frequency of the eigenmode was made equal to the frequency of the atomic transition.

The interaction of atoms with the electromagnetic field will be treated here in a semiclassical manner with the atoms described in terms of the quantum-mechanic Bloch equations and the field in terms of the classical Maxwell equation. Dissipation effects are not taken into account in this model. In other words, we consider a Hamiltonian dynamical system. Of course, this imposes restrictions on the characteristic time constants of the system.

If the density of atoms in the cavity volume V is sufficiently large, it is necessary to take into account the

interaction of atoms with their own radiation field. The corresponding criterion is the following:

$$\omega_c \geq \Omega_0 \,, \tag{2}$$

where

$$\omega_c = \sqrt{\frac{2\pi N d^2 \omega}{\hbar V}} \tag{3}$$

is the cooperative Rabi frequency [4], which characterizes the periodic energy exchange between N atoms and the field,

$$\Omega_0 = \frac{dE_0}{\hbar} \tag{4}$$

is the single-atom Rabi frequency, and E_0 is the maximum strength of the radiation field.

The semiclassical Hamiltonian of our model is given by

$$H = \frac{1}{2}\hbar\omega \sum_{j=1}^{N} \sigma_z^j + dE \sum_{j=1}^{N} \sigma_x^j \,, \tag{5}$$

where E is now not a prescribed field as in [1], but is a self-consistent field which satisfies the following single-mode Maxwell equation written in an approximation of slowly varying envelopes:

$$\frac{d^2E}{dt^2} + \omega^2 E = 4\pi\omega^2 d \frac{N}{V} \langle \sigma_x \rangle \,. \tag{6}$$

Let x, y, and z be the densities of the expectation values of the Pauli operators σ_x, σ_y, and σ_z, respectively:

$$x = N^{-1}\langle \sum \sigma_x \rangle, \quad y = N^{-1}\langle \sum \sigma_y \rangle, \quad z = N^{-1}\langle \sum \sigma_z \rangle \,. \tag{7}$$

These expectation values are defined with respect to the atomic initial state, which is assumed to be the same for all atoms. From the Heisenberg equations of motion follow the Bloch equations:

$$\begin{aligned} \frac{dx}{dt} &= -\omega y \,, \\ \frac{dy}{dt} &= \omega x - 2d\hbar^{-1} E z, \\ \frac{dz}{dt} &= 2d\hbar^{-1} E y \,. \end{aligned} \tag{8}$$

The components of the Bloch vector $(x\,, y\,, z)$ may be written in terms of the probability amplitudes $c_1(t)$ and $c_2(t)$ for the lower and upper states of an jth atom, respectively, as

$$\begin{aligned} x &= N^{-1} \sum (c_1^* c_2 + c_1 c_2^*) \,, \\ y &= N^{-1} i \sum (c_1^* c_2 - c_1 c_2^*) \,, \\ z &= N^{-1} \sum (|c_2|^2 - |c_1|^2) \,. \end{aligned} \tag{9}$$

Let us introduce the dimensionless time $\tau = \omega t$ and represent the field in the form

$$E(t) = E_0 e(t) \,, \quad 0 \leq e(t) \leq 1 \,, \tag{10}$$

where $e(t)$ is the dimensionless alternating component of the field. Now we can rewrite Eqs. (6) and (8) in the dimensionless Maxwell–Bloch form

$$\begin{aligned} \dot{x} &= -y\,, \\ \dot{y} &= x - 4\Omega e z\,, \\ \dot{z} &= 4\Omega e y\,, \\ \dot{e} &= -p\,, \\ \dot{p} &= e - \frac{\Lambda}{4\Omega}x\,. \end{aligned} \tag{11}$$

Dot denotes throughout the paper derivatives with respect to τ.

We have defined two control parameters, namely, the dimensionless separate Rabi frequency

$$\Omega = \frac{\Omega_0}{2\omega} \tag{12}$$

and the constant of the coupling between N atoms and a self-consistent field

$$\Lambda = \frac{8\pi N d^2}{\hbar V \omega}\,. \tag{13}$$

It follows from Eqs. (3) and (13) that the cooperative control parameter Λ is related to the dimensionless cooperative Rabi frequency in the following way:

$$\Lambda = \left(\frac{2\omega_c}{\omega}\right)^2. \tag{14}$$

Dynamical system (11) has two conservation laws

$$\begin{aligned} x^2 + y^2 + z^2 &= 1\,, \\ e^2 + p^2 - \frac{\Lambda}{2\Omega}ex - \frac{\Lambda}{8\Omega^2}z &= \text{const}\,. \end{aligned} \tag{15}$$

Conservation of the norm of the Bloch vector implies simply conservation of total probability for two-level atoms. The second law in Eq. (15) means conservation of total energy in a coupled atom–field system. It should be stressed that a rotating-wave approximation would lead to a third integral of motion reflecting conservation of the interaction energy. Without a rotating-wave approximation, we have three independent real variables [five variables in Eq. (11) minus two conservation laws (15)], which is the minimum required for chaos.

It was first found in [5] that the interaction of an ensemble of two-level atoms with their own radiation field can become chaotic when the cooperative parameter Λ exceeds a critical value $\Lambda_c \simeq 1$. Since the criterion for validity of the rotating-wave approximation is

$$\sqrt{\Lambda} \ll 1\,, \tag{16}$$

chaos arises when this approximation is no longer valid. The regime of dynamical chaos in the Maxwell–Bloch system and in its modifications has been investigated in a number of studies [6–10]. In particular, it was shown in [10] that in the case of driving a cavity by an additional external amplitude-modulated field chaos becomes possible even in the context of the rotating-wave approximation under certain conditions imposed on the detuning from resonance and on the amplitude of the external field.

The aim of our numerical experiments was to study the transition from order to chaos in Maxwell–Bloch model (11). With this in mind, we carefully investigated the dependence of the maximum Lyapunov exponent

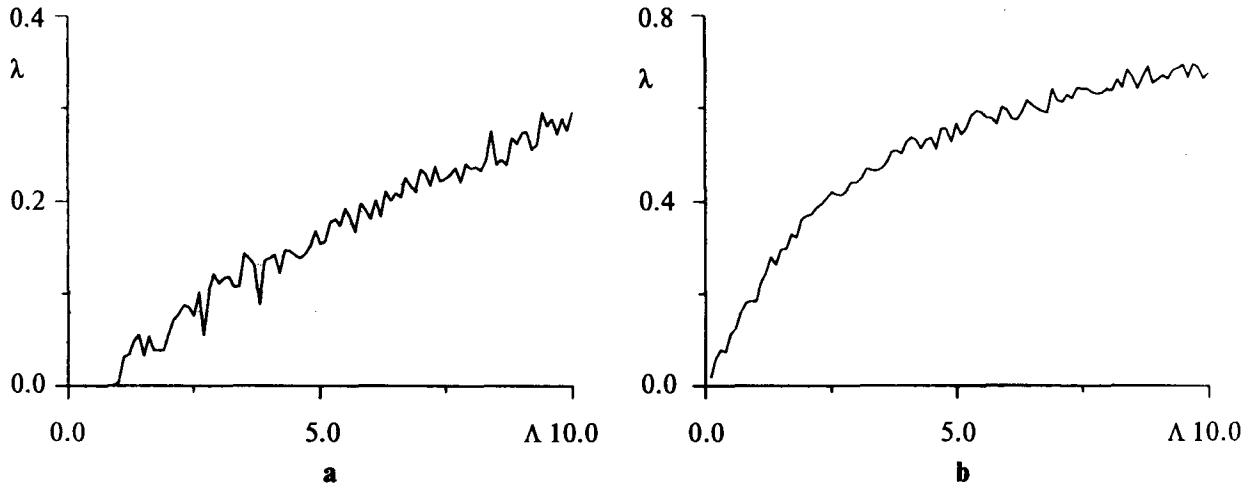

Fig. 1. The maximum Lyapunov exponent λ for Maxwell–Bloch system (11) as a function of the cooperative control parameter Λ for initially lower-state atoms (a) and for initially upper-state atoms (b). In both cases, $\Omega = 0.25 \cdot 10^{-6}$ and $e(0) = 1$, $p(0) = 0$.

λ of dynamical system (11) on both the control parameters Ω and Λ under the following initial conditions for the field:

$$e(0) = 1\,, \quad p(0) = 0\,. \tag{17}$$

As to atoms, we considered the two limiting cases in which all the atoms are assummed to be initially either in the lower state

$$x(0) = y(0) = 0\,, \quad z(0) = -1\,, \tag{18}$$

or in the upper state

$$x(0) = y(0) = 0\,, \quad z(0) = 1\,. \tag{19}$$

We found the maximum Lyapunov exponent to be an increasing function of the cooperative control parameter Λ [see Eq. (13)] on average. This is illustrated in Fig. 1 for initially unexcited atoms (Fig. 1a) and for initially excited ones (Fig. 1b). In both cases, the individual control parameter was $\Omega = 0.25 \cdot 10^{-6}$. In accordance with other studies [5, 7, 8], we have found that the Maxwell–Bloch system becomes chaotic (Fig. 1a) in the neighbourhood of $\Lambda_c \simeq 1$ for initially unexcited atoms (18). For initially excited atoms (19), chaos becomes evident for much smaller values of the cooperative parameter, of the order of $\Lambda_c \simeq 0.1$.

Let us estimate whether it is possible to observe such a transition to deterministic chaos under actual experimental conditions. For a typical magnitude of the electric dipole moment $d = 10^{-18}$ cgs and optical frequency $\omega = 3 \cdot 10^{14}$ rad/s, the critical value $\Lambda_c \simeq 0.1$ is reached at an atomic density N/V of the order of 10^{21} cm^{-3}. To obtain $\Omega = 0.25 \cdot 10^{-6}$, the strength of the cavity electric field must be $E_0 \simeq 0.15$ cgse. Thus, the Maxwell–Bloch dynamical system can undergo transition to chaos at high but reasonable atomic densities. As the cooperative control parameter Λ is varied, there are no surprises in the dynamics. It becomes more and more chaotic, at least up to $\Lambda = 10$, showing a tendency to saturation. We have not observed any transition to order with subsequent recurrence of chaos in the range considered $\Lambda_c < \Lambda \leq 10$.

A different onset of chaos was found for the dependence of the maximum Lyapunov exponent λ on the separate control parameter Ω, which is simply the dimensionless single-atom Rabi frequency (12). The results for a fixed value of the cooperative parameter $\Lambda = 1$ are shown in Fig. 2. Unlike the dependence $\lambda(\Lambda)$, the maximum Lyapunov exponent is not a monotonic function of the individual control parameter Ω. It has

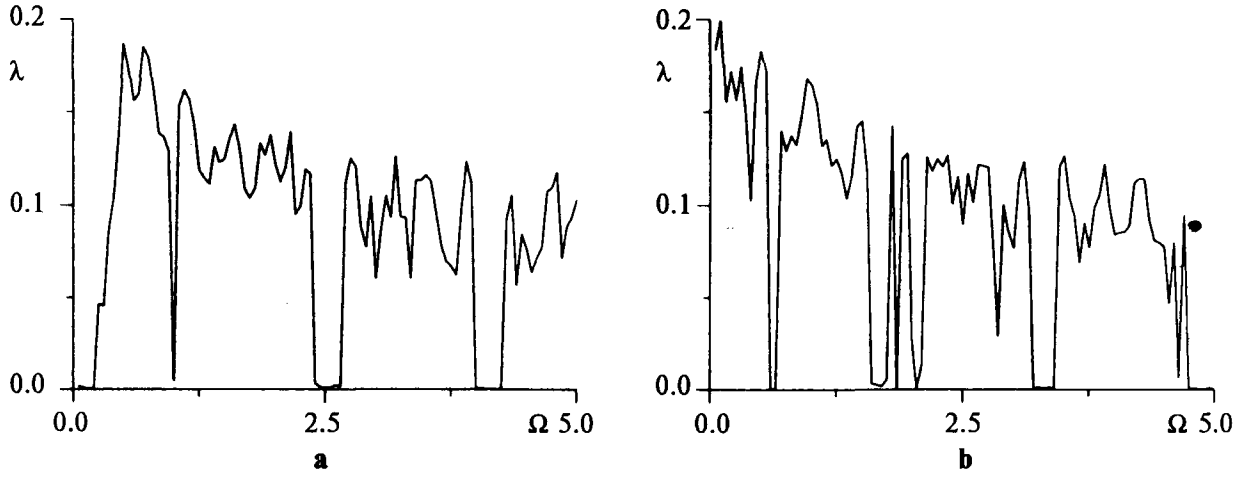

Fig. 2. The maximum Lyapunov exponent λ for Maxwell–Bloch system (11) as a function of the individual control parameter Ω for initially lower-state atoms (a) and for initially upper-state atoms (b). In both cases $\Lambda = 1$ and $e(0) = 1$, $p(0) = 0$.

both domains of positive values and those of negligibly small (zero) values. For both initially unexcited and excited atoms, the first transition to chaos occurs at $\Omega_c \simeq 0.1$. Summing up the results, we can state that, as the individual Rabi frequency increases, a sequence of transitions from quasi-periodicity to chaos takes place for two-level atoms interacting with a self-consistent radiation field in a cavity.

In principle, the dimensionless Rabi frequency (12) for optical transitions, say, with frequency $\omega = 3 \cdot 10^{14}$ rad/s, may vary within the following limits [11]:

$$10^{-7} \leq \Omega \leq 30 \,, \tag{20}$$

where the lower limit is determined by the typical energy-level width $\sim 10^7$ Hz, and the upper limit is connected to the atomic frequency $\sim 10^{17}$ rad/s. It follows from (12) that we need extremely strong electric fields, $E_0 \simeq 5 \cdot 10^4$ cgse, to reach the critical value $\Omega_c \simeq 0.1$.

2.2. Group-Theoretical Description of Semiclassical Dynamics

Let the Hamiltonian of N two-level atoms be again given by Eq. (5). Introducing the collective operators

$$R_0 = \frac{1}{2}\sum_{j=1}^{N} \sigma_z^j \,, \quad R_1 = \frac{1}{2}\sum_{j=1}^{N} \sigma_x^j \,, \quad R_2 = \frac{1}{2}\sum_{j=1}^{N} \sigma_y^j \tag{21}$$

and their combinations

$$R_\pm = R_1 \pm i R_2 \tag{22}$$

with the commutation relations

$$[R_0, R_\pm] = \pm R_\pm, \quad [R_+, R_-] = 2R_0 \,, \tag{23}$$

we can rewrite (5) as

$$H = \hbar\omega R_0 + \hbar\Omega_0 e(t)(R_+ + R_-) \,. \tag{24}$$

Here, the atomic Hamiltonian has exactly the same $SU(2)$ form as in Subsec. 2.1 of [1], and therefore the atomic subsystem is governed by the equation of motion (5) in [1], which now takes the form

$$\frac{d^2g}{dt^2} - \left(\frac{1}{e}\frac{de}{dt} + i\omega\right)\frac{dg}{dt} + (\Omega_0 e)^2 g = 0 , \tag{25}$$

where the single-atom Rabi frequency Ω_0 is given by Eq. (4), and $e(t)$ is the dimensionless alternating component of the electric field which satisfies the Maxwell equation

$$\frac{d^2E}{dt^2} + \omega^2 E = 4\pi\omega^2\mathcal{P} , \tag{26}$$

where the polarization $\mathcal{P}$ produced by atoms is

$$\mathcal{P} = \frac{Nd}{V}\left\langle\sum\sigma_x\right\rangle = \frac{Nd}{V}\langle R_+ + R_-\rangle . \tag{27}$$

It is convenient to use the same dimensionless control parameters Ω and Λ as in Subsec. 2.1 [see Eqs. (12) and (13)]. Then the dimensionless versions for atomic subsystem (25) and for field subsystem (26) are of the form

$$\begin{aligned} \ddot{g} - \left(\frac{\dot{e}}{e} + i\right)\dot{g} + (2\Omega e)^2 g &= 0 , \\ \ddot{e} + e - \frac{\Lambda}{4\Omega}\langle R_+ + R_-\rangle &= 0 , \end{aligned} \tag{28}$$

where the expectation values of the collective operators

$$\langle R_+ + R_-\rangle = \mathrm{Sp}\left[U\varrho_0 U^\dagger (R_+ + R_-)\right] \tag{29}$$

can be calculated for any initial density matrix ϱ_0 using the evolution operator (4) in [1].

Restricting ourselves to pure states and using the results of Subsec. 2.3 in [1], we have the following solution of the time-dependent Schrödinger equation for the probability amplitudes

$$\begin{bmatrix} c_2(t) \\ c_1(t) \end{bmatrix} = \begin{bmatrix} e^{-i\omega t/2} & 0 \\ 0 & e^{i\omega t/2} \end{bmatrix} \begin{bmatrix} g & -\tilde{g}^* \\ \tilde{g} & g^* \end{bmatrix} \begin{bmatrix} c_2(0) \\ c_1(0) \end{bmatrix} , \tag{30}$$

where c_1 and c_2 are the probability amplitudes for the lower and upper states, respectively. The expectation value $\langle R_+ + R_-\rangle$ can be written in terms of these amplitudes:

$$\langle R_+ + R_-\rangle = c_1(t)c_2^*(t) + c_2(t)c_1^*(t) . \tag{31}$$

Thus, we have two coupled oscillators (28) describing the self-consistent interaction between two-level atoms and a single-mode classical field. Let us introduce real variables:

$$u \equiv \mathrm{Re}\, g , \quad v \equiv \mathrm{Im}\, g , \quad \tilde{u} \equiv \mathrm{Re}\,(\tilde{g}e^{i\omega t}) , \quad \tilde{v} \equiv \mathrm{Im}\,(\tilde{g}e^{i\omega t}) . \tag{32}$$

In view of (30) and (31), one can express the expectation value $\langle R_+ + R_-\rangle$ for any pure state in terms of these variables. For instance, it has the form

$$\langle R_+ + R_-\rangle_- = -2(u\tilde{u} + v\tilde{v}) \tag{33}$$

for atoms that are initially in lower states. For initially excited atoms, we have

$$\langle R_+ + R_- \rangle_+ = 2(u\tilde{u} + v\tilde{v}) \,. \tag{34}$$

Now we may represent Eqs. (28) in the form of first-order dimensionless equations for the real variables:

$$\begin{aligned} \dot{u} &= 2\Omega e\tilde{v} \,, \\ \dot{v} &= -2\Omega e\tilde{u} \,, \\ \dot{\tilde{u}} &= -\tilde{v} + 2\Omega ev \,, \\ \dot{\tilde{v}} &= \tilde{u} - 2\Omega eu \,, \\ \dot{e} &= -p \,, \\ \dot{p} &= e \pm \frac{\Lambda}{2\Omega}(u\tilde{u} + v\tilde{v}) \end{aligned} \tag{35}$$

with the two conservation laws

$$\begin{aligned} u^2 + v^2 + \tilde{u}^2 + \tilde{v}^2 &= 1 \,, \\ e^2 + p^2 \pm \frac{\Lambda}{\Omega} e(u\tilde{u} + v\tilde{v}) \pm \frac{\Lambda}{8\Omega^2}(u^2 + v^2 - \tilde{u}^2 - \tilde{v}^2) &= \text{const} \,. \end{aligned} \tag{36}$$

Introducing new real variables

$$\begin{aligned} x &= \mp(u\tilde{u} + v\tilde{v}) \,, \\ y &= \pm(\tilde{u}v - u\tilde{v}) \,, \\ z &= \pm(\tilde{u}^2 + \tilde{v}^2 - u^2 - v^2) \,, \end{aligned} \tag{37}$$

we can rewrite set (35) exactly in Maxwell–Bloch form (11). The respective integrals of motion (15) follow from integrals (36) with substitution of (37). In Eqs. (35)–(37), the upper signs refer to initially unexcited atoms and the lower signs refer to initially excited atoms.

3. The onset of Dynamical Chaos in Neoclassical Model of Atom–Field Interaction

3.1. Jaynes–Cummings Dynamical System

In this section we start with the fully quantized N-atom Jaynes–Cummings Hamiltonian

$$H = \frac{1}{2}\hbar\omega \sum_{j=1}^{N} \sigma_z^j + \hbar\omega \left(a^\dagger a + \frac{1}{2} \right) + \hbar\Lambda_0 (a + a^\dagger) \sum_{j=1}^{N} \sigma_x^j \,, \tag{38}$$

where

$$\Lambda_0 = \frac{dE_{\text{vac}}}{\hbar} \tag{39}$$

is the vacuum Rabi angular frequency for resonance interaction. The vacuum electric field E_{vac} (or the electric field per photon) is given by the known expression (see, e.g., [12])

$$E_{\text{vac}} = \sqrt{\frac{2\pi\hbar\omega}{V}} \,. \tag{40}$$

The vacuum Rabi frequency Λ_0 has the meaning of the frequency of population oscillations for a two-level system in a vacuum field given by (40). The cooperative Rabi frequency, which was introduced in Subsec. 2.1. [see Eq. (3)], is related to Λ_0 as

$$\omega_c = \Lambda_0 \sqrt{N} \, . \tag{41}$$

Without resorting to a rotating-wave approximation, we can use the Heisenberg equations of motion with the Hamiltonian (38) to obtain the following set of equations for the atomic and the field operators:

$$\begin{aligned}
i\frac{d}{dt}\sum\sigma_x &= -i\omega\sum\sigma_y \, , \\
i\frac{d}{dt}\sum\sigma_y &= i\omega\sum\sigma_x - 2i\Lambda_0(a+a^\dagger)\sum\sigma_z \, , \\
i\frac{d}{dt}\sum\sigma_z &= 2i\Lambda_0(a+a^\dagger)\sum\sigma_y \, , \\
i\frac{d}{dt}a &= \omega a + \Lambda_0\sum\sigma_x \, , \\
i\frac{d}{dt}a^\dagger &= -\omega a^\dagger - \Lambda_0\sum\sigma_x \, .
\end{aligned} \tag{42}$$

The crucial point is factorization of these equations. We merely average Eqs. (42) and uncouple the operator products as follows:

$$\langle a\sigma\rangle = \langle a\rangle\langle\sigma\rangle \, . \tag{43}$$

Introducing the dimensionless time $\tau = \omega t$, we obtain the following closed set of first-order equations for the neoclassical model of field–atom interaction:

$$\begin{aligned}
\dot{x} &= -y \, , \\
\dot{y} &= x + 4\Lambda_N E z \, , \\
\dot{z} &= -4\Lambda_N E y \, , \\
\dot{E} &= -P \, , \\
\dot{P} &= E - 4\Lambda_N x \, ,
\end{aligned} \tag{44}$$

where we have introduced the expectation values for the field operators:

$$E = -\frac{1}{\sqrt{N}}\langle a + a^\dagger\rangle \, , \quad P = -i\frac{1}{\sqrt{N}}\langle a - a^\dagger\rangle \tag{45}$$

in addition to the atomic expectation values x, y, and z given by Eq. (7).

The control parameter in neoclassical model (44) has the form

$$\Lambda_N = \frac{\Lambda_0\sqrt{N}}{2\omega} \equiv \frac{\omega_c}{2\omega} \, . \tag{46}$$

This parameter is related to the cooperative control parameter of semiclassical Maxwell–Bloch model (13) in a simple way:

$$\Lambda = (4\Lambda_N)^2 \, . \tag{47}$$

System (44) has two conservation laws:

$$\begin{aligned}
x^2 + y^2 + z^2 &= 1 \, , \\
E^2 + P^2 + 2z + 8\Lambda_N E x &= \text{const} \, .
\end{aligned} \tag{48}$$

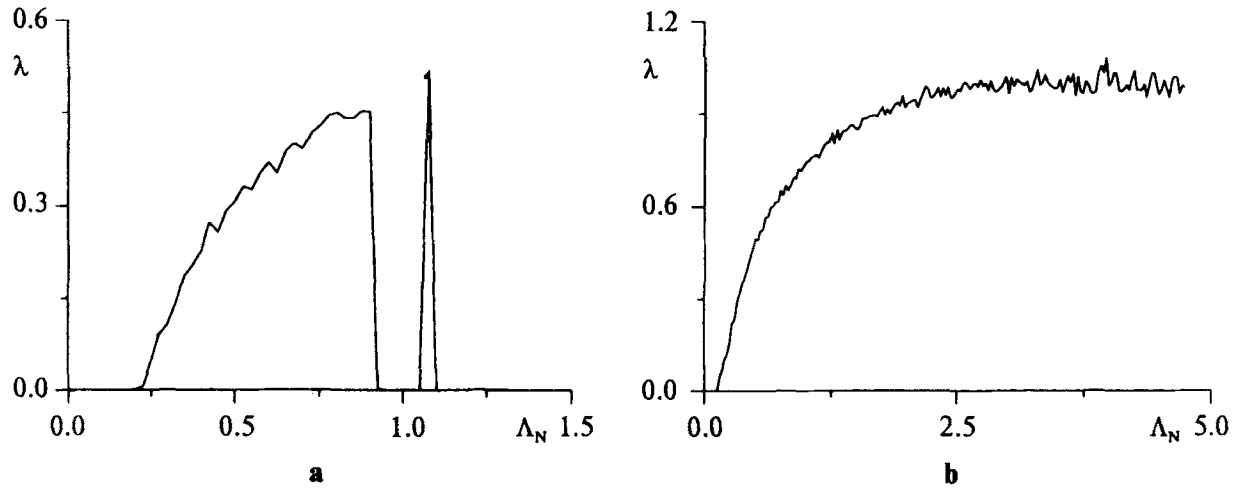

Fig. 3. The maximum Lyapunov exponent λ for Jaynes–Cummings system (44) as a function of the cooperative control parameter Λ_N for initially lower-state atoms (a) and for initially upper-state atoms (b). In both cases, $E(0) = 1$, $P(0) = 0$.

As in the Maxwell–Bloch case, we would have had an extra conservation law if we had resorted *ab initio* to a rotating-wave approximation.

To analyze chaos, we again examine the dependence of the maximum Lyapunov exponent λ of neoclassical Jaynes–Cummings system (44) on the control parameter Λ_N of this system [13]. The results are shown in Fig. 3a for initially unexcited atoms

$$x(0) = y(0) = 0\,, \quad z(0) = -1\,, \quad E(0) = 1\,, \quad P(0) = 0 \tag{49}$$

and in Fig. 3b for initially excited atoms

$$x(0) = y(0) = 0\,, \quad z(0) = 1\,, \quad E(0) = 1\,, \quad P(0) = 0\,. \tag{50}$$

It is evident that the onsets of chaos are different in these two cases. With initially unexcited atoms (Fig. 3a) the system exhibits a complicated sequence of order–chaos–order–chaos... transitions with alternating regular and irregular modes. In the case of initially excited atoms, the system becomes more and more chaotic with increasing Λ_N (see Fig. 3b).

To elucidate the role that atomic initial states play in the onset of dynamical chaos, we plotted the map of chaos as a function of the value of the control parameter Λ_N and of the initial atomic inversion $z(0)$ [14]. It follows from the first conservation law in (48) that the atomic transition dipole moment is equal to zero for the largest $z(0) = 1$ and the smallest $z(0) = -1$ values of population inversion. When $|z(0)| \neq 1$ the atoms have nonzero transition dipole moments and, therefore, are in a superposition state. Figure 4 demonstrates the results of calculations. Curves in Fig. 4 are the lines of equal values of the maximum Lyapunov exponent. The more shaded an area in this figure, the stronger the chaos for the corresponding values of Λ_N and $z(0)$.

We conclude from this map that a coupled atom–field system in a neoclassical approximation remains regular up to large values of the control parameter Λ_N if atoms were prepared in superposition states with closed probabilities to be found at lower and upper levels, i.e. with $z(0) \approx 0$. A sea of chaos can be seen on the map under conditions of unbalanced initial probabilities.

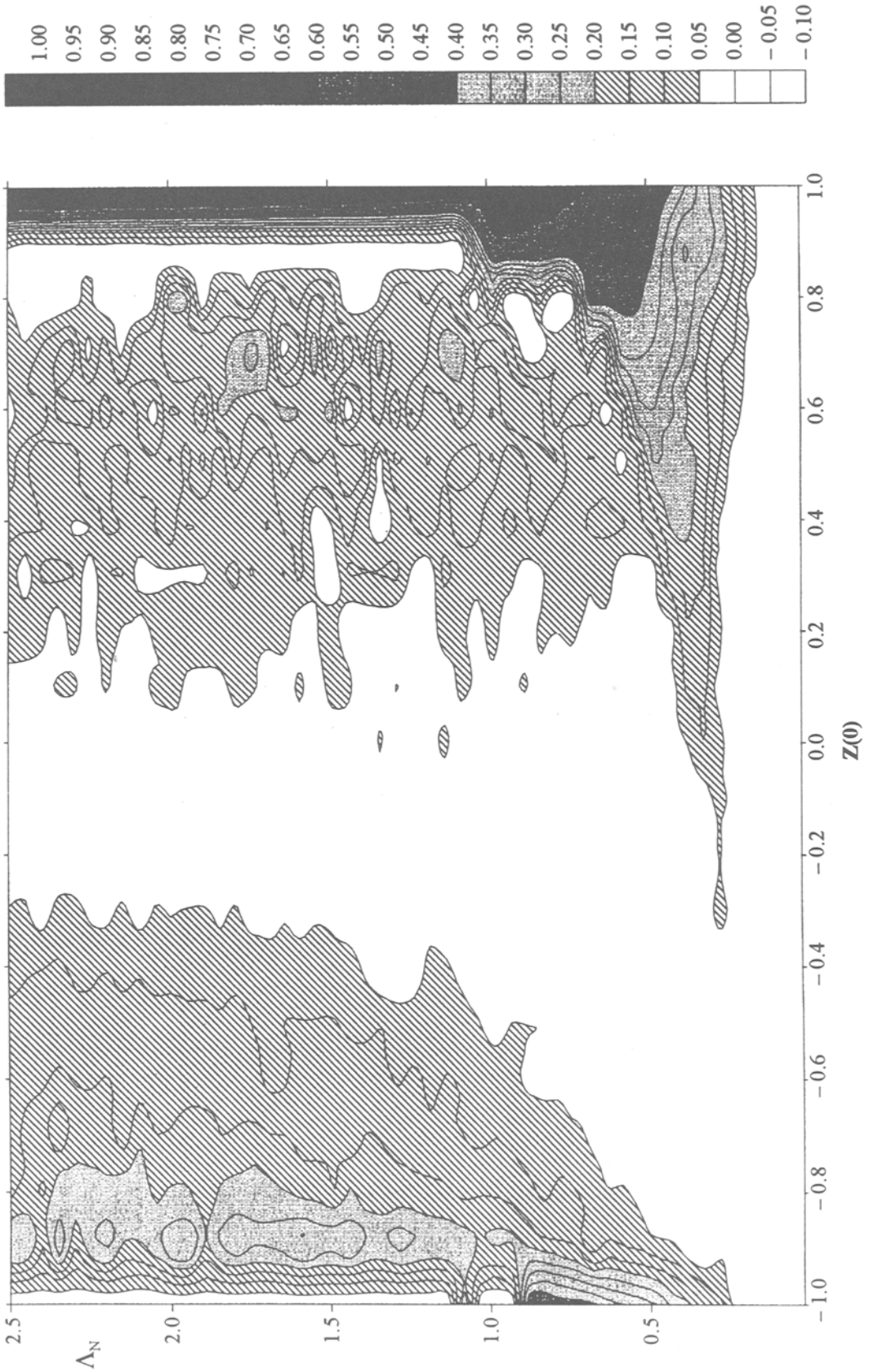

Fig. 1. Map of dynamical chaos for Jaynes–Cummings system (44) in coordinates of the cooperative control parameter Λ_N and the initial population inversion $z(0)$. The initial conditions for the field are the same as in Fig. 3.

3.2. Group-Theoretical Description of Neoclassical Dynamics

Dynamical system (44) can be rewritten in terms of $SU(2)$ variables (32). For initially unexcited atoms, it has the form

$$\begin{aligned} \dot{u} &= 2\Lambda_N E\tilde{v}\,, \\ \dot{v} &= -2\Lambda_N E\tilde{u}\,, \\ \dot{\tilde{u}} &= -\tilde{v} + 2\Lambda_N E v\,, \\ \dot{\tilde{v}} &= \tilde{u} - 2\Lambda_N E u\,, \\ \dot{E} &= -P\,, \\ \dot{P} &= E + 8\Lambda_N(u\tilde{u} + v\tilde{v})\,. \end{aligned} \tag{51}$$

While the form of standard neoclassical dynamical system (44) does not depend on the initial conditions, the system for group-theoretical variables does depend on the atomic initial conditions [compare Eqs. (33) and (34)]. For completeness, we write here the integrals of motion for system (51)

$$\begin{aligned} u^2 + v^2 + \tilde{u}^2 + \tilde{v}^2 &= 1\,, \\ E^2 + P^2 + 4\Lambda_N E(u\tilde{u} + v\tilde{v}) + u^2 + v^2 - \tilde{u}^2 - \tilde{v}^2 &= \text{const}\,. \end{aligned} \tag{52}$$

In the Maxwell–Bloch model, the variables u, v, $\tilde{u}$, and $\tilde{v}$ are parameters of the dynamical-symmetry group of the atom–field system, since its semiclassical Hamiltonian (5) generates an $SU(2)$ algebra. This is not the case for Jaynes–Cummings Hamiltonian (38), which generates *ab initio* an infinite-dimensional dynamical Lie algebra. Nevertheless, one may treat these unknowns as new real variables in a neoclassical approximation.

Numerical experiments were carried out with dynamical system (51) using the fourth-order Runge–Kutta method [15] under the following initial conditions:

$$u(0) = 0\,, \quad v(0) = 1\,, \quad \tilde{u}(0) = 0\,, \quad \tilde{v}(0) = 0\,, \quad E(0) = 1\,, \quad P(0) = 0\,. \tag{53}$$

This is the case of initially unexcited atoms. It was found that the behavior of the largest Lyapunov exponent λ as a function of Λ_N was exactly the same as in Fig. 3a. It is seen in this figure that there are both domains of positive values of λ, where the system is chaotic, and those of negligibly small (zero) values of λ, where it exhibits (quasi)regular motion.

To obtain more comprehensive information about the motion of a coupled atom–field system, we calculated the power spectra and phase portraits for three values of the coupling constant Λ_N corresponding to three different types of motion. The following representative values of Λ_N were chosen:

- Domain of regular motion with $\Lambda_N = 0.15$ and $\lambda = 0$.
- Domain of quasi-regular motion with $\Lambda_N = 0.95$ and $\lambda = 0$.
- Domain of chaotic motion with $\Lambda_N = 0.68$ and $\lambda \simeq 0.4$.

The power spectra for regular and quasi-regular motion feature a δ-like structure (Figs. 5a and 5b) and become broadened in the case of chaotic motion (Fig. 5c). Two-dimensional projections of the system's phase portraits onto the plane $\mathrm{Im}\, g = v$ – $\mathrm{Re}\, g = u$ of the atomic variables are displayed in Fig. 6 for all three representative values of the coupling constant. The corresponding projections onto the plane $P - E$ of the field variables are shown in Fig. 7.

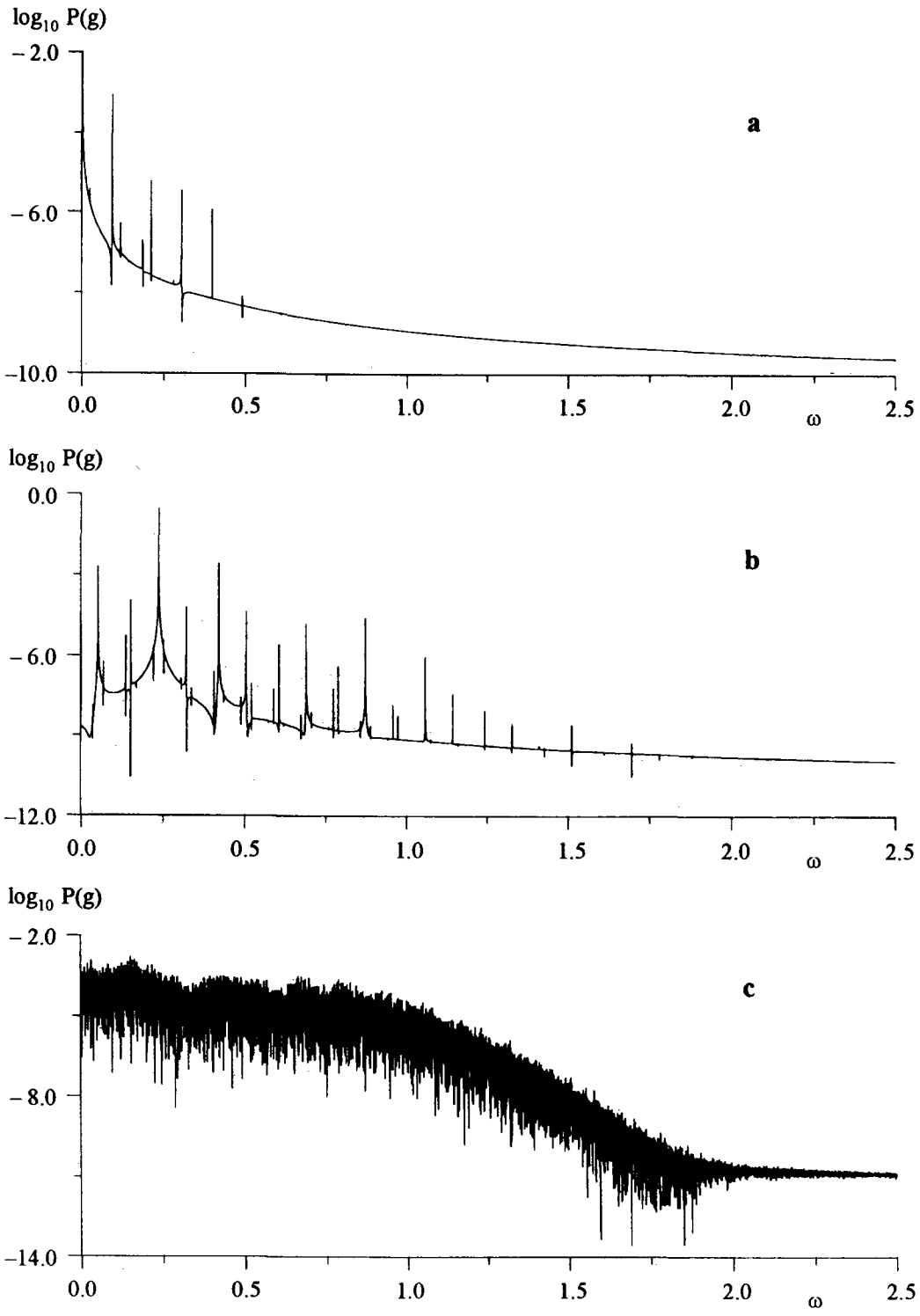

Fig. 5. Power spectra for group-theoretical version (51) of the Jaynes–Cummings system in the cases of regular motion with $\Lambda_N = 0.15$ (a), quasi-regular motion with $\Lambda_N = 0.95$ (b), and chaotic motion with $\Lambda_N = 0.68$ (c). The initial conditions for the field are the same as in Fig. 3.

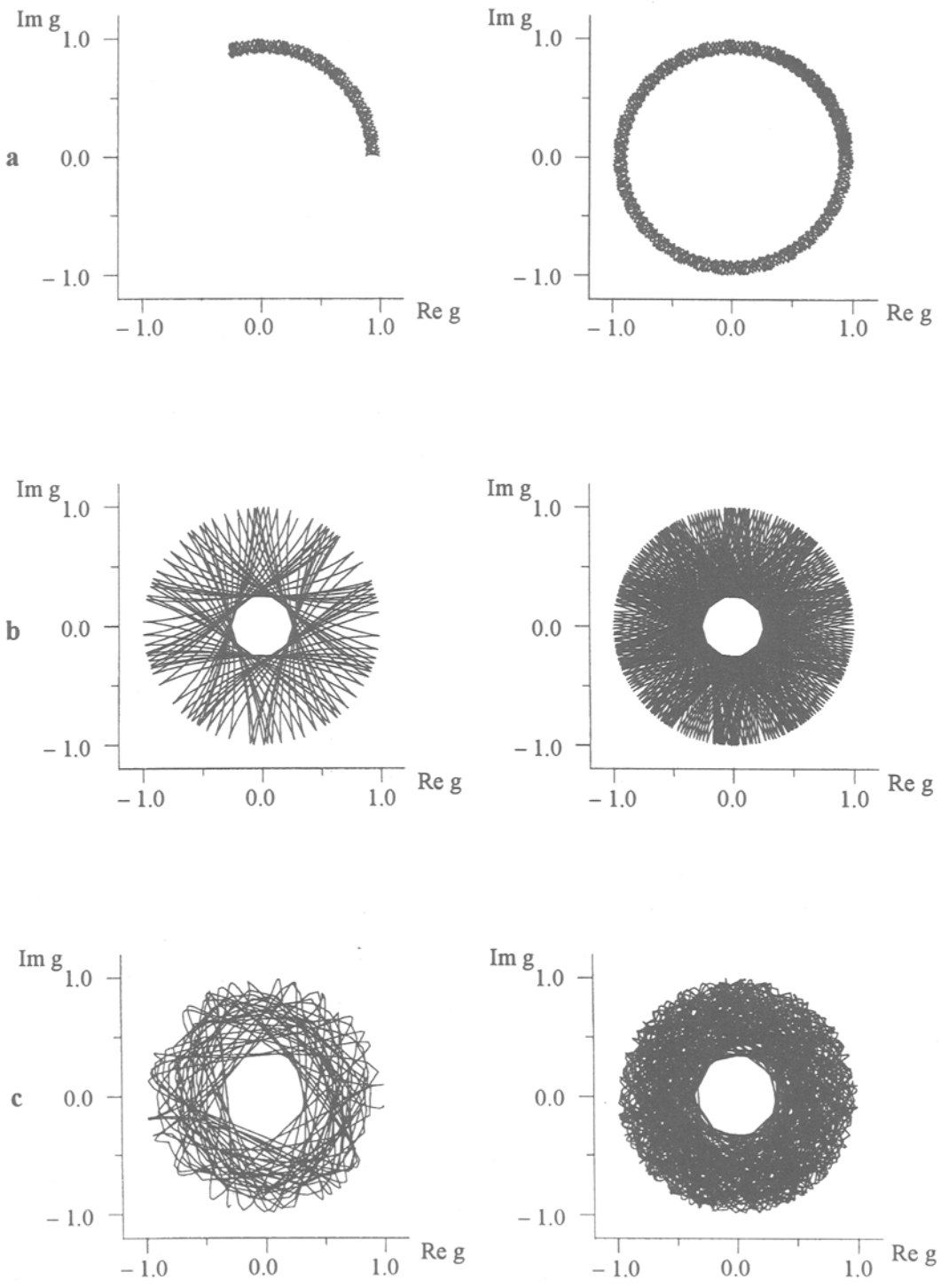

Fig. 6. Stroboscopic two-dimensional projections of the phase portrait for group-theoretical version (51) of the Jaynes–Cummings system onto the plane of the $SU(2)$ group parameter in the cases of regular motion with $\Lambda_N = 0.15$ (a), quasi-regular motion with $\Lambda_N = 0.95$ (b), and chaotic motion with $\Lambda_N = 0.68$ (c). The initial conditions for the field are the same as in Fig. 3.

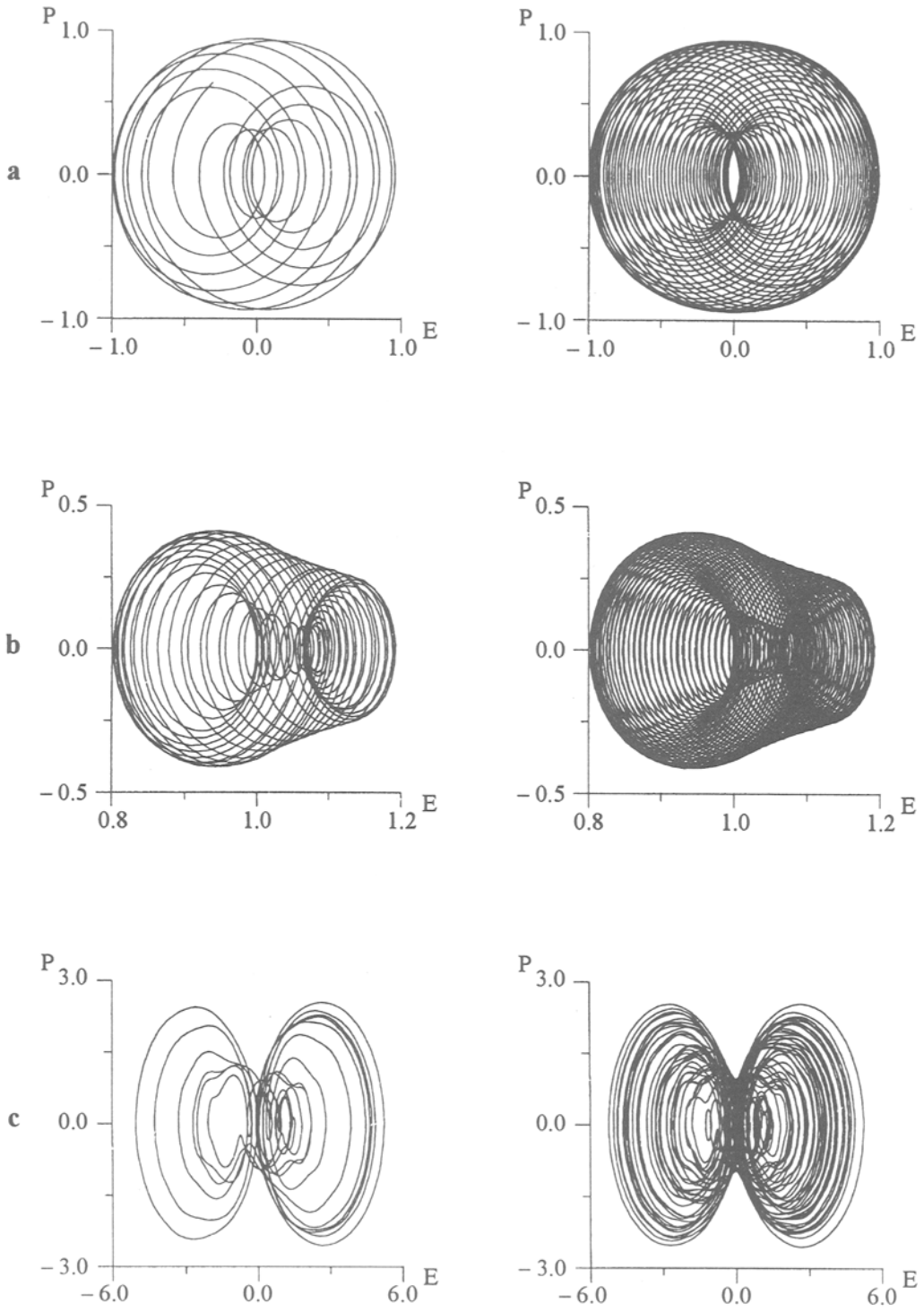

Fig. 7. Stroboscopic two-dimensional projections of the phase portrait for group-theoretical version (51) of the Jaynes–Cummings system onto the plane of the field variables in the cases of regular motion with $\Lambda_N = 0.15$ (a), quasi-regular motion with $\Lambda_N = 0.95$ (b), and chaotic motion with $\Lambda_N = 0.68$ (c). The initial conditions for the field are the same as in Fig. 3.

4. Actual Quantum Electrodynamical Systems with Strong Coupling

The purpose of this section is to discuss different types of actual quantum electrodynamical systems with large values of the vacuum Rabi frequency Λ_0 (39), characterizing the radiator–field coupling, and to select the most promising candidates for experimental investigations of transitions to dynamical chaos, which were discovered numerically in the preceding sections. As follows from our numerical results, transition to chaos in the Jaynes–Cummings model takes place when the control parameter Λ_N, which is related to Λ_0 by Eq. (46) exceeds a certain critical value Λ_c which depends on the initial conditions. We found its minimum value to be equal to $\simeq 0.1$ for initially excited atoms (see Fig. 3b). Let us determine whether it is possible to reach this order of magnitude for Λ_N in actual physical systems. For convenience, we introduce the single-atom control parameter

$$\Lambda_1 = \frac{\Lambda_0}{2\omega} . \tag{54}$$

It follows from Eq. (46) that $\Lambda_N = \Lambda_1\sqrt{N}$.

4.1. Atoms in Cavities

We begin our discussion with atom–field systems in electromagnetic resonators operating in the strong coupling regime, which are widely used in resonator quantum electrodynamics [16–18]. In this regime, the atom–field coupling is much larger than the reciprocals of all other characteristic times such as the lifetimes of atoms and the cavity field and the atom–field interaction time.

Rydberg atoms are very good objects for the study of quantum electrodynamical effects in the microwave region. In typical experiments [18], rubidium atoms with transition frequency $\omega/2\pi = 51.1$ GHz (between two adjacent states with principal quantum numbers $n = 50$ and $n = 51$) and the transition electric dipole moment $d = 1250\ D$ are placed in an electromagnetic resonator with a typical size of 1 cm and an effective volume of the order of 0.1 cm^3. The vacuum electric field (40) is equal to $E_{\text{vac}} \simeq 1.3 \cdot 10^{-7}$ cgse. The vacuum Rabi frequency (39) then reaches $\Lambda_0 \simeq 2 \cdot 10^5$ rad/s; values of this order are maximal for Rydberg atoms in microwave cavities. Therefore, the highest attainable value of the single-atom control parameter for these objects is of the order of $\Lambda_1 \simeq 3 \cdot 10^{-7}$.

Strong coupling can also be achieved in the optical region. Especially strong atom–field coupling is observed at the surface of small dielectric spheres [19]. For instance, the whispering-gallery mode at the surface of a silica microsphere of 17.5 μm radius has a very high Q-factor and a frequency, $\omega/2\pi \simeq 4 \cdot 10^{14}$ Hz, which is almost in resonance with the rubidium $5S - 5P_{3/2}$ transition ($d \simeq 2\ D$). The effective mode volume is $V \simeq 1.6 \cdot 10^{-10}$ cm^3, which yelds the vacuum electric field $E_{\text{vac}} \simeq 0.3$ cgse. The vacuum Rabi frequency is then of the order of $\Lambda_0 \simeq 6 \cdot 10^8$ rad/s. Therefore, the single-atom control parameter for such an object reaches $\Lambda_1 \simeq 10^{-7}$.

Thus, we see that the highest attainable value of Λ_1 for atoms in both the microwave and optical regions, is of the order of 10^{-7}. As follows from Eq. (54), in this case one needs $N = 10^{12}$ atoms to reach the critical value of the cooperative control parameter Λ_N, of the order of 10^{-1}, which is the threshold for transition to dynamical chaos in the Jaynes–Cummings neoclassical model.

4.2. Microcavity Polaritons

An interesting quantum electrodynamical system with very strong coupling is that of quantum-well excitons in integrated semiconductor microcavities [20–23]. We will discuss here quantum wells located in a

Fabri–Perot semiconductor microcavity that is formed by two distributed Bragg reflectors placed one wavelength of light apart. For definiteness, we consider the structure of an actual $AlAs/Al_{0.4}Ga_{0.6}As$ sample used in experiments (see, e.g. [20]). The lifetime of this microcavity and its resonance width are 130 fs and 5 Mev, respectively. A quantum well width of the order of 76 Å ensures an exciton transition that is resonant with the cavity mode at 785 nm at temperatures of 5–10 K. At such temperatures, the relaxation time of quantum-well excitons is $T_2 = 1$ ps, and the radiative lifetime is approximately 10 ps [20]. Such quantum electrodynamical effects as spontaneous emission enhancement and suppression, vacuum Rabi oscillations, and vacuum Rabi splitting have been observed with excitons in semiconductor microcavities (for reviews see [20, 21]).

The exciton states of a quantum well form a two-dimensional band. On the other hand, a resonant Fabri–Perot cavity also has a two-dimensional density of photon modes. Because of the conservation of the wave vector of an exciton in its interaction with light [22] a given excitonic state can interact only with a wave-vector-matched cavity photon state. As a result, normal modes of the exciton–cavity system, which can be termed "cavity polaritons," arise.

In the strong coupling regime, it is possible to describe cavity polaritons by Jaynes–Cummings Hamiltonian (38). The Pauli matrices now describe two excitonic states, and the creation and annihilation operators describe a cavity field which is assumed to be a single mode one. All the analytical and numerical results of Sec. 3 are valid for our cavity–polariton system (in the context of a two-level approximation). In particular, different onsets of chaos become possible when the control parameter exceeds a critical value (see Figs. 3 and 4).

Let us estimate the vacuum Rabi frequency (39) for the structure considered. The relevant dipole moment is [20]

$$d = er_a|F|L\,, \tag{55}$$

where er_a is the atom-like dipole moment,

$$|F|^2 = \frac{8}{\pi a_0^3} \tag{56}$$

is the probability per unit area of finding an electron and a hole in the same unit cell, and L is the characteristic size of the crystal. Using Eqs. (39) and (40), the vacuum Rabi frequency can be written as

$$\Lambda_0 = er_a\sqrt{\frac{\omega n}{\hbar l_{\rm cav}}|F(0)|^2}\,, \tag{57}$$

where $l_{\rm cav}$ is the effective cavity length. For a sample with $|F(0)|^2 = 1.6\cdot 10^{12}$ cm^{-2}, $r_a = 6$ Å, $l_{\rm cav} = 785$ nm, $e = 4.8\cdot 10^{-10}$ cgse and with $n = 25$ quantum wells, we have $\Lambda_0 \simeq 2\cdot 10^{13}$ rad/s. Such a high vacuum Rabi frequency yields a value of the individual control parameter of the order of $\Lambda_1 \simeq 5\cdot 10^{-3}$, which is far in excess of the coupling constants for atom–field systems (see Subsec. 4.1). It is worthwhile to mention that the estimated magnitudes of Λ_0 for other fabricated semiconductor structures can reach $(1–3)\cdot 10^{13}$ rad/s [23].

To sum up, we can say that quantum-well excitons in semiconductor microcavities are good objects for study of the quantum signatures of dynamical chaos because of their very strong coupling to cavity modes.

Acknowledgments

I thank L. E. Kon'kov for aid in the numerical calculations. This work was partially supported by the International Science Foundation and the Russian Government under Grants Nos. NZ7000 and NZ7300 and by the Russian Foundation for Basic Research under Grant No. 96-02-19827.

References

1. S. V. Prants, *J. Rus. Laser Res.*, **17**, 539 (1996).
2. A. Lichtenberg and M. Lieberman, *Regular and Stochastic Motion*, Springer, New York (1983).
3. E. T. Jaynes and F. W. Cummings, *Proc IEEE.*, **51**, 89 (1963).
4. R. U. Dicke, *Phys. Rev.*, **93**, 99 (1956).
5. P. I. Belobrov, G. M. Zaslavskii, and G. Kh. Tartakovskii, *Zh. Éksp. Teor. Fiz.*, **71**, 1799 (1976).
6. V. S. Egorov and I. A. Chekhonin, *Zh. Tekh. Fiz.*, **56**, 572 (1986).
7. J. R. Ackerhalt, P. W. Milonni, and M.-L. Shih, *Phys. Rep.*, **128**, 205 (1985).
8. R. F. Fox and J. C. Eidson, *Phys. Rev. A*, **34**, 482 (1986).
9. J. C. Eidson and R. F. Fox, *Phys. Rev. A*, **34**, 3288 (1986).
10. K. N. Alekseev and G. P. Berman, *Zh. Éksp. Teor. Fiz.*, **92**, 1985 (1987).
11. N. B. Delone, *Interaction of Laser Radiation with Matter: Course of Lectures* [in Russian], Nauka, Moscow (1989).
12. L. Allen and J. H. Eberly, *Optical Resonance and Two-Level Atoms*, Wiley, New York (1975).
13. S. V. Prants and L. E. Kon'kov, *Kvantov. Élektron.*, **23**, N 1 (1996).
14. S. V. Prants and L. E. Kon'kov, *Izv. Acad. Nauk, Ser. Fiz.*, N 3 (1996).
15. L. E. Kon'kov and S. V. Prants, *J. Math. Phys.*, **37**, N 2 (1996).
16. P. R. Berman (ed.), *Cavity Quantum Electrodynamics*, Academic Press, Boston (1994).
17. O. Benson, G. Raithel and H. Walter, *Phys. Rev. Lett.*, **72**, 3506 (1994).
18. J. M. Raymond and S. Haroche, in: E. Burstein and C. Weisbuch (eds.), *Confined Electrons and Photons*, Plenum Press, New York (1995).
19. F. Treussart, J. Hare, L. Collot, et al., *Opt. Lett.*, **19**, 1653 (1994).
20. T. B. Norris, in: E. Burstein and C. Weisbuch (eds.), *Confined Electrons and Photons*, Plenum Press, New York (1995).
21. D. A. B. Miller, in: E. Burstein and C. Weisbuch (eds.), *Confined Electrons and Photons*, Plenum Press, New York (1995).
22. J. J. Hopfield, *Phys. Rev.*, **112**, 1555 (1958).
23. G. Bjork, S. Pau, J. Jacobson, and Y. Yamamoto, *Phys. Rev. B*, **50**, 17336 (1994).